

Synchrotron powder diffraction data for some smectite clay mineral standards

Joel W. Reid ^{a)}

Canadian Light Source, 44 Innovation Boulevard, Saskatoon, SK S7N 2V3, Canada

(Received 10 April 2023; accepted 7 July 2023)

Synchrotron powder diffraction data is presented for a series of relatively phase-pure smectite clay mineral standards obtained from the Clay Minerals Society. Rietveld refinement using a model for turbostratic disorder was performed to estimate the lattice parameters and mineral impurities in the smectite standards. Bragg reflection lists and raw data have been provided for inclusion in the Powder Diffraction File.

© The Author(s), 2023. Published by Cambridge University Press on behalf of International Centre for Diffraction Data.

[doi:10.1017/S0885715623000283]

Key words: smectite, nontronite, montmorillonite, powder diffraction, Rietveld refinement

I. INTRODUCTION

Clay minerals are notable for both their importance to a broad array of industries (Harvey and Murray, 1997) and the significant challenges they present for correct identification, characterization, and quantification (Moore and Reynolds, 1989). Clays are layered phyllosilicates that are difficult to analyze due to their presence in complex heterogeneous mixtures, extensive faulting and disorder, layer swelling and contraction with water content, and a propensity for preferred orientation. Smectite clays in particular are challenging to physically model due to the presence of turbostratic disorder, where adjacent layers are randomly translated and rotated with respect to one another (Ufer et al., 2004; Gilg et al., 2020), giving rise to patterns with anisotropic broadening and asymmetric peak shapes. These features make smectite powder diffraction patterns difficult to adequately describe with a traditional *d*-spacing–intensity (*d*-*I*) list.

Synchrotron data collection with a capillary in transmission, particularly using a large two-dimensional (2D) detector, can provide some advantages for examination of mineralogical and clay samples. Capillary mounting with rotation during data collection and azimuthal integration of full 2D data sets are excellent strategies for minimizing both preferred orientation (clays) and graininess (quartz and other coarse minerals), making it easier to obtain accurate intensity estimates from challenging, heterogeneous samples.

The Powder Diffraction File (PDF; Gates-Rector and Blanton, 2019) began including raw diffraction data with experimental entries, when available, in PDF-4+ in 2008. The inclusion of raw data with PDF entries significantly improves the description of disordered, poorly crystalline, and amorphous materials like clays and polymers, facilitating better identification. Raw data deposited in the PDF has even been used to solve the crystal structures of pharmaceuticals

that were previously unpublished (Reid et al., 2016; Reid and Kaduk, 2021). This work used synchrotron powder diffraction data to examine four relatively phase-pure smectite clay mineral standards obtained from the Clay Minerals Society (CMS) to provide high-quality powder patterns for the PDF. The patterns were examined with Rietveld refinement to determine their lattice parameters, estimate the crystalline phase compositions, and to aid indexing of the Bragg peaks.

II. EXPERIMENT

The smectite clay mineral standards examined in this work were obtained from the CMS and are summarized in Table I. Nominal chemical formulas obtained from previous studies (Van Olphen and Fripiat, 1979; Keeling et al., 2000) were assumed for the clays. Samples were ground with an agate mortar and pestle, and specimens were mounted in 0.3 mm ID polyimide capillaries for data collection.

Powder X-ray diffraction (PXRD) patterns were collected using the Canadian Macromolecular Crystallography Facility bend magnet beamline 08B1-1 (Fodje et al., 2014) at the Canadian Light Source (CLS). 08B1-1 is a bending magnet beamline with a Si (111) double crystal monochromator. 2D diffraction patterns were collected on a Pilatus3 S 6M detector with an active area of 423.6 mm × 434.6 mm. The patterns were collected at an energy of 18 keV ($\lambda = \sim 0.6888$ Å) and a sample-detector distance of ~ 350 mm.

The 2D PXRD patterns were calibrated and integrated using the GSASII software package (Toby and Von Dreele, 2013). The sample-detector distance, detector centering, tilt, and wavelength were calibrated using a series of patterns obtained from a lanthanum hexaboride (LaB₆) standard reference material (NIST SRM 660a LaB₆) and the calibration parameters were applied to all patterns. After calibration, the 2D patterns were integrated to obtain standard point detector powder diffraction patterns. Three to six short exposure 2D patterns (1 or 2 min) were obtained for each clay sample, to

^{a)} Author to whom correspondence should be addressed. Electronic mail: joel.reid@lightsource.ca



TABLE I. The smectite clay mineral standards examined in this work.

CMS Code	Mineral Name	Chemical Formula (Reference)
NAu-1	Nontronite	$M_{1.05}^+[Al_{0.29}Fe_{3.68}Mg_{0.04}][Si_{6.98}Al_{1.02}]O_{20}(OH)_4$ (Keeling et al., 2000)
NAu-2	Nontronite	$M_{0.72}^+[Fe_{3.83}Mg_{0.05}][Si_{7.55}Al_{0.45}]O_{20}(OH)_4$ (Keeling et al., 2000)
SAz-2	Montmorillonite	$(Ca_{0.39}Na_{0.36}K_{0.04})[Al_{2.71}Mg_{1.11}Fe_{0.12}Mn_{0.01}Ti_{0.03}][Si_{8.00}]O_{20}(OH)_4$ (Van Olphen and Fripiat, 1979)
STx-1b	Montmorillonite	$(Ca_{0.27}Na_{0.04}K_{0.01})[Al_{2.41}Fe_{0.09}Mg_{0.71}Ti_{0.03}][Si_{8.00}]O_{20}(OH)_4$ (Van Olphen and Fripiat, 1979)

ensure that no hydration changes were taking place during data collection. Search/match phase identification was performed on the smectite clay patterns using the Powder Diffraction File, PDF-4+ (Gates-Rector and Blanton, 2019) to determine the mineral impurities.

Rietveld refinements were performed on the patterns using the BGMN software program (Bergmann et al., 1998) via the Profex graphical user interface (Döbelin and Kleeberg, 2015). BGMN uses a fundamental parameters approach for peak shape definition which was primarily

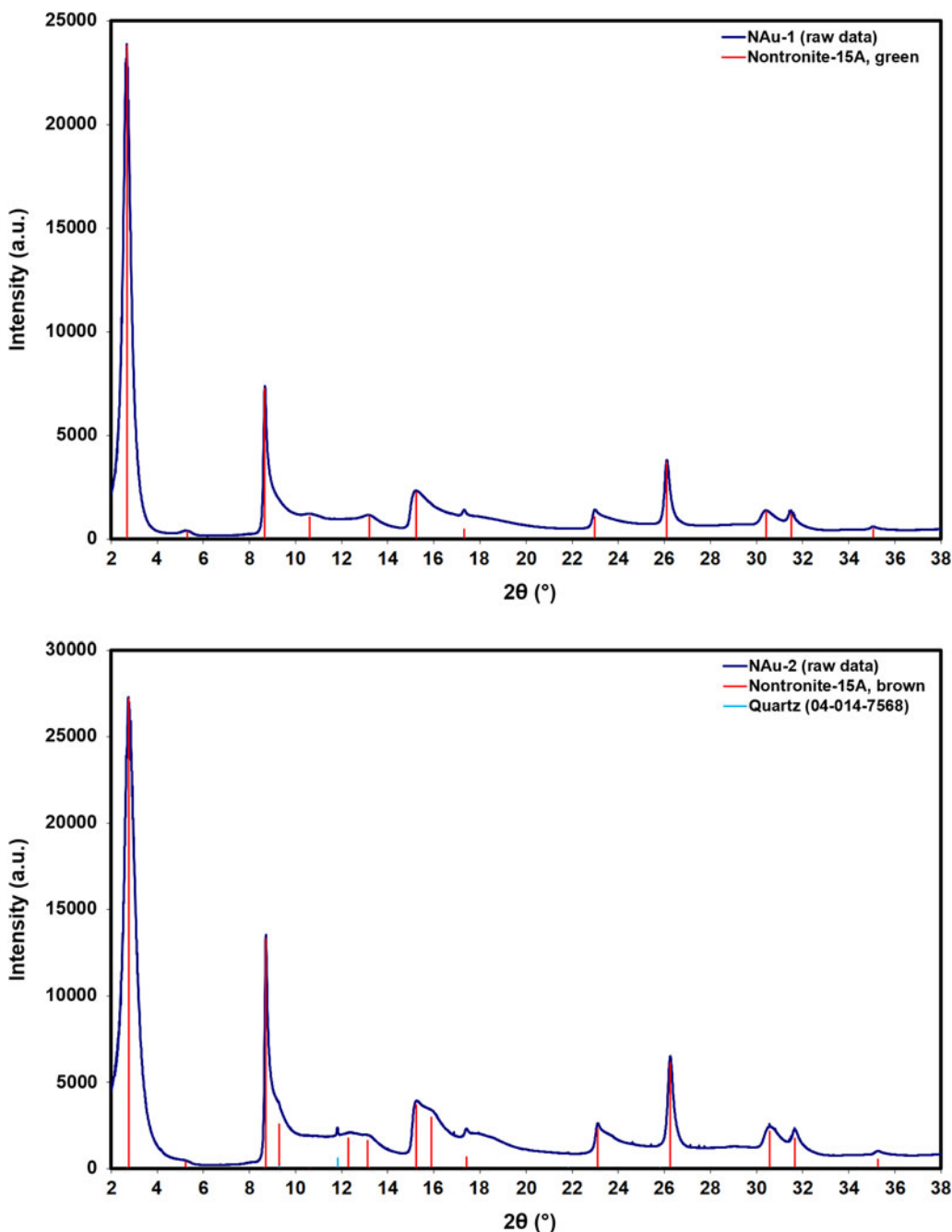


Figure 1. Plots of the raw data and Bragg reflections for the observed phases in the nontronite samples, NAu-1 (top) and NAu-2 (bottom).

designed for laboratory diffractometers. Establishment of appropriate instrument parameters for the synchrotron beamline was an iterative, empirical exercise. Optical elements of a previous synchrotron instrument parameter file (Döbelin, 2019) were modified in small increments and compiled at each step, to iteratively obtain a satisfactory starting description of the instrument parameters using a diffraction pattern from NIST SRM 660a LaB₆.

Rietveld refinements of the smectite clay data sets employed a turbostratic disorder model for smectite (Ufer et al., 2004, 2008) using tetrahedral-octahedral-tetrahedral (TOT) layer coordinates determined by electron diffraction (Tsipursky and Drits, 1984). Modifications were made to the starting octahedral and tetrahedral site occupations (based on the chemical formulas in Table I) for individual samples.

Minor deviations were allowed in the occupations during refinement using hard limits on refined occupancies and constraints on total site occupation for individual sites.

III. RESULTS AND DISCUSSION

The powder patterns for the smectite clay minerals are illustrated with phase identification and indexing results in Figure 1 (nontronite samples NAu-1 and NAu-2) and Figure 2 (montmorillonite samples SAz-2 and STx-1b). While NAu-1 appeared phase-pure, minor impurities were observed in NAu-2 (quartz) and SAz-2 (quartz and feldspar). In addition to quartz and feldspar, STx-1b contained a large, broad peak attributable to opal or cristobalite. This was consistent with previous baseline powder diffraction studies of this

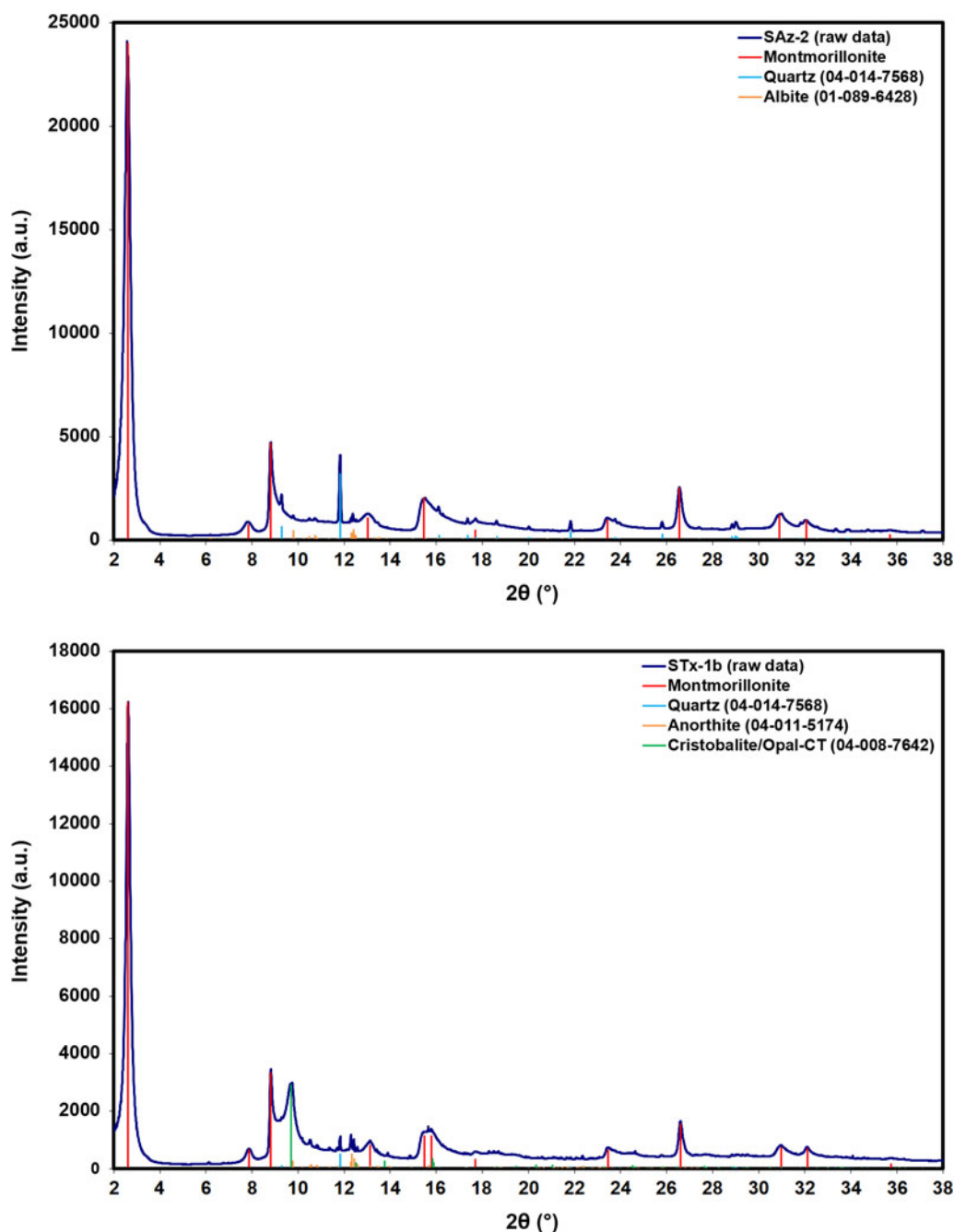


Figure 2. Plots of the raw data and Bragg reflections for the observed phases in the montmorillonite samples, SAz-2 (top) and STx-1b (bottom).

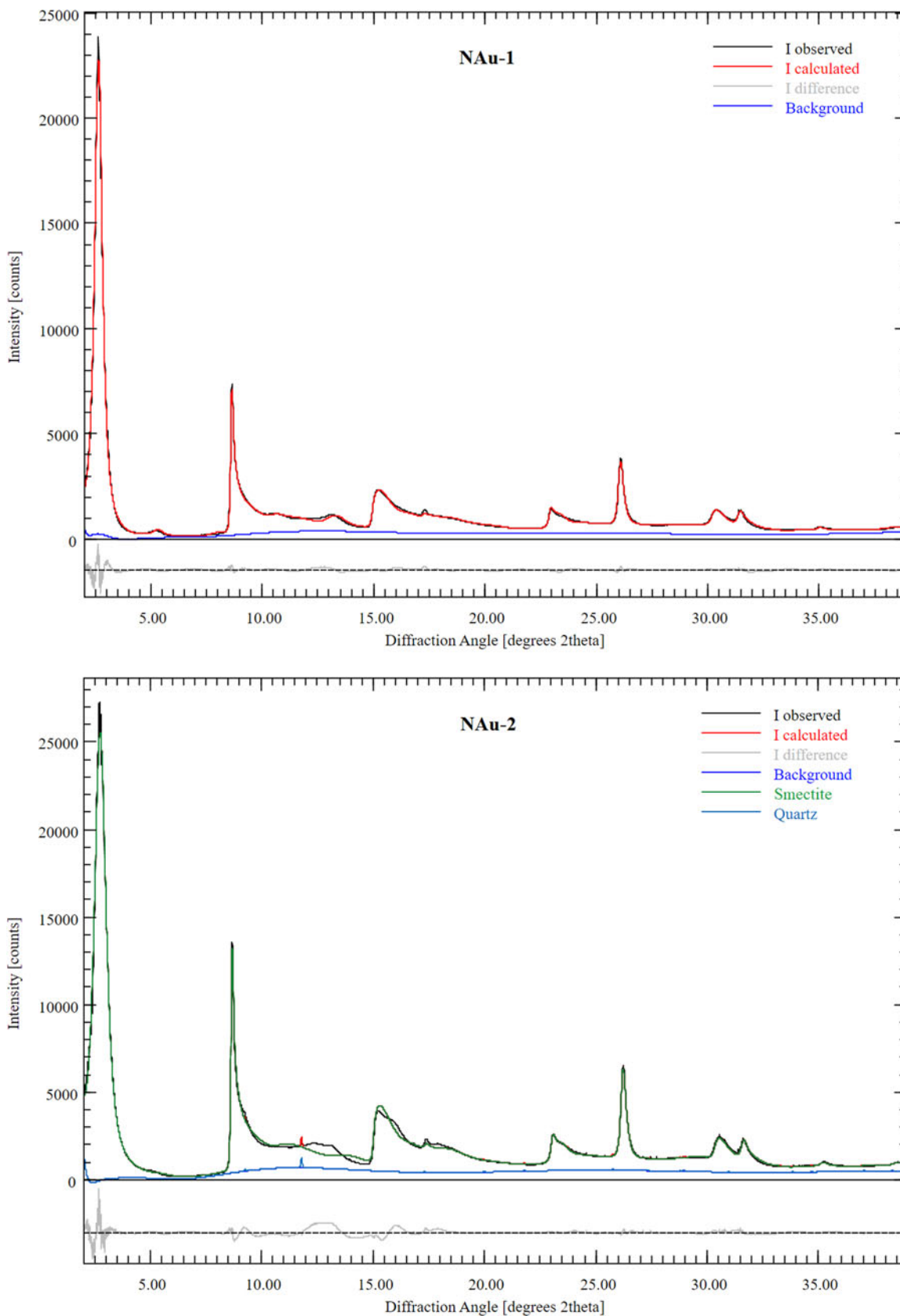


Figure 3. Plots of the final Rietveld refinements obtained for the nontronite samples, N Au-1 (top) and N Au-2 (bottom).

clay, where the peak was attributed to opal-CT (Chipera and Bish, 2001).

Rietveld refinements are illustrated for the four data sets in Figure 3 (nontronite samples N Au-1 and N Au-2) and Figure 4

(montmorillonite samples SAz-2 and STx-1b), and the lattice parameters, refinement indices, and mineral impurity contents are summarized in Table II. The refinement for the phase-pure N Au-1 yielded a β -angle very close to 100.4° . It was generally

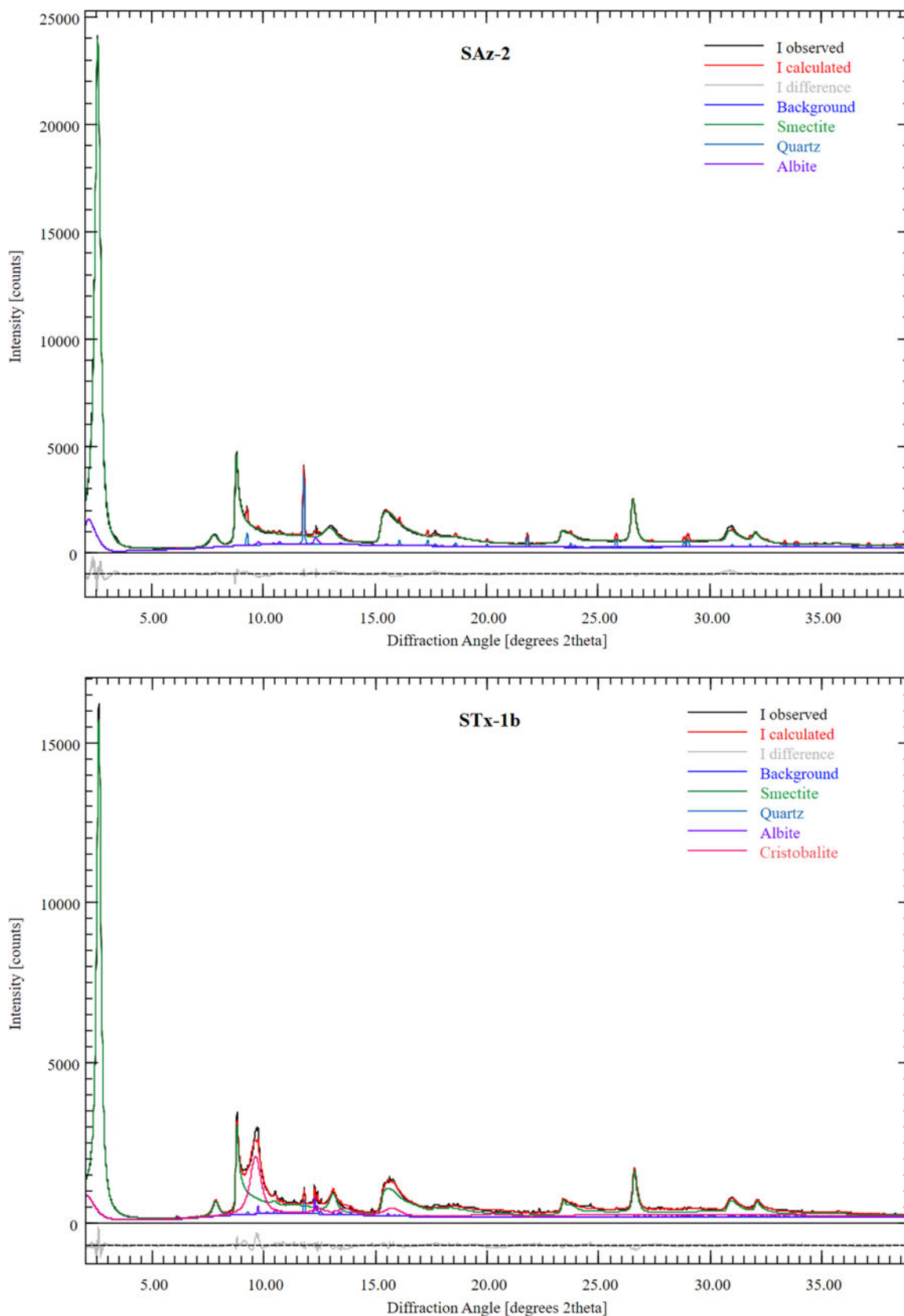


Figure 4. Plots of the final Rietveld refinements obtained for the montmorillonite samples, SAz-2 (top) and STx-1b (bottom).

found that refining the β -angle resulted in minimal improvement to the refinements, but increased the estimated standard deviations in the lattice parameters. The β -angle was subsequently fixed at 100.4° for all four refinements. The a and b

lattice parameters are larger in the nontronites than the montmorillonites, consistent with higher iron content in the octahedral sheets. The cis-trans site occupancies in the octahedral sheets refined to completely cis-vacant (NAu-1, NAu-2, and

TABLE II. The Rietveld-refined unit cell parameters for the smectite clays examined in this work, obtained using Profex/BGMN.

CMS Code	NAu-1	NAu-2	SAz-2	STx-1b
Symmetry	Monoclinic	Monoclinic	Monoclinic	Monoclinic
a (Å)	5.2894(12)	5.2681(20)	5.2027(12)	5.1937(15)
b (Å)	9.1784(17)	9.1157(30)	9.0052(19)	8.9973(24)
c (Å)	15.0924(50)	14.5432(87)	15.4530(33)	15.3413(35)
β (°)	100.4	100.4	100.4	100.4
R_{wp} (%)	5.23	7.72	5.00	6.02
R_{exp} (%)	2.94	2.25	3.25	4.11
Impurities	None	Quartz (<1 wt.%)	Quartz (4 wt.%), feldspar (2 wt.%)	Quartz (1 wt.%), feldspar (3 wt.%), opal/cristobalite (24 wt.%)

STx-1b) or predominantly cis-vacant (trans occupancy of 0.956(9) for SAz-2) for all refinements, consistent with most smectite clay minerals (Tsipursky and Drits, 1984; Gilg et al., 2020).

Three of the Rietveld refinements were excellent in terms of refinement indices and visually reasonable fits, but the refinement for NAu-2 was clearly inferior to the other three. The smectite model was unable to fully account for some of the features observed between ~ 10 and 18° in the experimental data set (Figure 3, bottom). The refinement was still suitable for estimating the lattice parameters and the quartz impurity content (<1 wt.%), which were the primary purposes in this work.

For the Rietveld refinement with the STx-1b data set, the opal/cristobalite phase was modeled using cristobalite with significant peak broadening. While this may not be a completely physically correct representation of the opal-CT phase, broadened cristobalite provided a reasonable fit yielding a phase composition that was consistent with previously reported results (Chipera and Bish, 2001).

Unit cells, Bragg reflection lists, and raw data for all four clays were provided in CIF format for inclusion in the PDF database. Three of the Bragg reflection lists (NAu-1, SAz-2, and STx-1b) were indexed consistent with turbostratic disorder considered as completely uncorrelated stacking (Ufer et al., 2004), where all reflections belong to either $\{hk0\}$ (h or k can be zero) or $\{00l\}$ sets. NAu-2 required deviation from completely uncorrelated stacking to account for a small number of Bragg reflections.

IV. DEPOSITED DATA

Crystallographic Information Framework (CIF) files containing unit cells, d -spacing–intensity lists and raw data were deposited with ICDD. The data can be requested at pdj@icdd.com.

ACKNOWLEDGEMENTS

Many thanks to Nicola Döbelin for providing the starting synchrotron instrument resolution file and his suggestions for obtaining a suitable description of the beamline profile. The author also thanks the Canadian Light Source for a small project grant which facilitated the purchase of the CMS clay mineral standards.

Research described in this paper was performed using beamline 08B1-1 at the Canadian Light Source, which is supported by the Canadian Foundation for Innovation, the Natural Sciences and Engineering Research Council of Canada, the National Research Council Canada, the Canadian Institutes

of Health Research, the Government of Saskatchewan, Western Economic Diversification Canada, and the University of Saskatchewan.

CONFLICT OF INTEREST

The author has no conflict of interest to declare.

REFERENCES

- Bergmann, J., P. Friedel, and R. Kleeberg. 1998. "BGMN—A New Fundamental Parameters Based Rietveld Program for Laboratory X-Ray Sources, Its Use in Quantitative Analysis and Structure Investigations." *CPD Newsletter* 20 (5): 5–8.
- Chipera, S. J., and D. L. Bish. 2001. "Baseline Studies of the Clay Minerals Society Source Clays: Powder X-Ray Diffraction Analyses." *Clays and Clay Minerals* 49 (5): 398–409.
- Döbelin, N. 2019 Personal Communication.
- Döbelin, N., and R. Kleeberg. 2015. "Profex: A Graphical User Interface for the Rietveld Refinement Program BGMN." *Journal of Applied Crystallography* 48 (5): 1573–1580.
- Fodje, M., P. Grochulski, K. Janzen, S. Labiuk, J. Gorin, and R. Berg. 2014. "08B1-1: An Automated Beamline for Macromolecular Crystallography Experiments at the Canadian Light Source." *Journal of Synchrotron Radiation* 21 (3): 633–637.
- Gates-Rector, S., and T. Blanton. 2019. "The Powder Diffraction File: A Quality Materials Characterization Database." *Powder Diffraction* 34 (4): 352–360.
- Gilg, H. A., S. Kaufhold, and K. Ufer. 2020. "Smectite and Bentonite Terminology, Classification, and Genesis." *Bentonites, Characterization, Geology, Mineralogy, Analysis, Mining, Processing and Uses* Geol. Jb. B 107, 1–18.
- Harvey, C. C., and H. H. Murray. 1997. "Industrial Clays in the 21st Century: A Perspective of Exploration, Technology and Utilization." *Applied Clay Science* 11 (5-6): 285–310.
- Keeling, J. L., M. D. Raven, and W. P. Gates. 2000. "Geology and Characterization of Two Hydrothermal Nontronites from Weathered Metamorphic Rocks at the Uley Graphite Mine, South Australia." *Clays and Clay Minerals* 48 (5): 537–548.
- Moore, D. M., and R. C. Reynolds Jr. 1989. *X-Ray Diffraction and the Identification and Analysis of Clay Minerals*. Oxford University Press (OUP), New York.
- Reid, J. W., and J. A. Kaduk. 2021. "Crystal Structure of Donepezil Hydrochloride Form III, $C_{24}H_{29}NO_3 \cdot HCl$." *Powder Diffraction* 36 (4): 233–240.
- Reid, J. W., J. A. Kaduk, and M. Vickers. 2016. "The Crystal Structure of Trandolapril, $C_{24}H_{34}N_2O_5$: An Example of the Utility of Raw Data Deposition in the Powder Diffraction File." *Powder Diffraction* 31 (3): 205–210.
- Toby, B. H., and R. B. Von Dreele. 2013. "GSAS-II: The Genesis of a Modern Open-Source All Purpose Crystallography Software Package." *Journal of Applied Crystallography* 46 (2): 544–549.
- Tsipursky, S. I., and V. A. Drits. 1984. "The Distribution of Octahedral Cations in the 2:1 Layers of Dioctahedral Smectites Studied by Oblique-Texture Electron Diffraction." *Clay Minerals* 19 (2): 177–193.

Ufer, K., G. Roth, R. Kleeberg, H. Stanjek, R. Dohrmann, and J. Bergmann. 2004. "Description of X-Ray Powder Pattern of Turbostratically Disordered Layer Structures with a Rietveld Compatible Approach." *Zeitschrift für Kristallographie-Crystalline Materials* 219 (9): 519–527.

Ufer, K., H. Stanjek, G. Roth, R. Dohrmann, R. Kleeberg, and S. Kaufhold. 2008. "Quantitative Phase Analysis of Bentonites by the Rietveld Method." *Clays and Clay Minerals* 56 (2): 272–282.

Van Olphen, H., and J. J. Fripiat. 1979. *Data Handbook for Clay Materials and Other Non-Metallic Minerals*. Pergamon Press, New York.